Structural Dynamics of the M4 Transmembrane Segment during Acetylcholine Receptor Gating

ARTICLE *in* STRUCTURE · NOVEMBER 2004

Impact Factor: 5.62 · DOI: 10.1016/j.str.2004.08.004 · Source: PubMed

3 AUTHORS, INCLUDING:

Ananya Mitra
Stanford University
8 PUBLICATIONS **422** CITATIONS

SEE PROFILE

Structure, Vol. 12, 1909–1918, October, 2004, ©2004 Elsevier Ltd. All rights reserved. DOI 10.1016/j.str.2004.08.004

Structural Dynamics of the M4 Transmembrane Segment during Acetylcholine Receptor Gating

Ananya Mitra, Timothy D. Bailey, and Anthony L. Auerbach*
Center for Single-Molecule Biophysics
Department of Physiology and Biophysics
State University of New York at Buffalo
Buffalo, New York 14214

Summary

The transition state structures that link the stable end states of allosteric proteins are largely unresolved. We used single-molecule kinetic analysis to probe the dynamics of the M4 transmembrane segments during the closed⇌open isomerization of the neuromuscular acetylcholine receptor ion channel (AChR). We measured the slopes (ϕ) of the free energy relationships for 87 mutants, which reveal the open- versus closed-like characters of the mutated residues at the transition state and hence the sequence and organization of gating molecular motions. ϕ was constant throughout the length of the α subunit M4 segment with an average value of 0.54, suggesting that this domain moves as a unit, approximately midway through the reaction. Analysis of a hybrid construct indicates that the two α subunits move synchronously. Between subunits, the sequence of M4 motions is α-ϵ-β. The AChR ion channel emerges as a dynamic nanomachine with many moving parts.

Introduction

The nicotinic acetylcholine receptor (AChR) is a ligand-gated ion channel that can switch between ion-impermeable and ion-permeable conformations. In the absence of transmitter, the closed (C) conformation is greatly favored, but in the presence of transmitter the open (O) form predominates. The driving energy for this change in relative occupancy is the $\sim 10^4$-fold higher affinity of open AChRs for two transmitter molecules (Auerbach, 2003; Changeux and Edelstein, 1998; Jackson, 1989; Karlin and Akabas, 1995; Sine, 2002).

AChRs are large membrane proteins ($\sim$300 kDa) and the C⇌O allosteric conformational change ("gating") is not instantaneous. Rather, the side chain and backbone motions that constitute diliganded AChR gating are highly asynchronous and propagate along the long axis of the protein approximately as a solitary "wave" (Grosman et al., 2000b). This conformational wave is coarse grained. The sequential movement of only a few discrete domains ("blocks") appears to be sufficient to couple the low⇌high-affinity change at the transmitter binding sites with the low⇌high-conductance change of the pore (Chakrapani et al., 2004). Here, we describe the participation of the M4 transmembrane segments, which lie in the periphery of the membrane domain, in this sequence of molecular movements.

AChRs have five homologous subunits that are arranged pseudosymmetrically about a central ion-conduction pathway (Karlin and Akabas, 1995; Unwin, 2000). The extracellular portion of each subunit is comprised mainly of β strands and connecting loops and houses two transmitter binding sites that each lie at a subunit interface (Blount and Merlie, 1989; Brejc et al., 2002; Celie et al., 2004; Chiara and Cohen, 1997; Sine and Claudio, 1991). The transmembrane portion of each subunit is comprised of four helical segments connected by one extracellular and two intracellular loops. The M2 transmembrane helix is closest and the M4 helix is furthest from the central axis (Miyazawa et al., 2003) (1UV6.pdb and 1OED.pdb; Figure 6C).

Both affinity-labeling (Blanton and Cohen, 1992, 1994) and structural studies (Miyazawa et al., 2003) show that M4 is an α helix that makes extensive contact with the lipid bilayer (Barrantes, 2002, 2003). Although M4 is far ($>$2.5 nm) from both the channel lumen and the transmitter binding sites, functional analyses have shown that mutations of some of the residues in the M4 segment of the α (Bouzat et al., 2000; Tamamizu et al., 1999), β (Lee et al., 1994; Ortiz-Miranda et al., 1997), and ϵ (Bouzat et al., 2002) subunits alter the diliganded gating equilibrium constant. These results suggest that these M4 residues experience a change in their local environment, i.e., move, during the gating reaction. Specifically, it appears that in the α subunit, a hydrogen bond involving the side chain at position T422 serves to increase the relative stability of the open conformation, whereas at the equivalent position in the ϵ subunit (S451), a hydrogen bond decreases the relative stability of the open conformation (Bouzat et al., 2000, 2002). The companion groups for these bonds (which may be within the AChR or the lipid bilayer) have not been identified, but candidates include residues in other transmembrane segments (Bouzat et al., 2000), phospholipid head groups (Bouzat et al., 1998), and steroids (Garbus et al., 2002).

We have examined the diliganded channel-opening and -closing rate constants from 88 different AChR constructs, having mutations of 21 different M4 residues, in all five subunits. The results indicate that, in the α subunits, the M4 segments move synchronously, near the middle of the gating reaction, after the α subunit extracellular domains and M2-M3 linkers but before the δ subunit M2 segment. The motions of the M4 domains of the ϵ and β subunits follow that of αM4, with no apparent motion in the δ subunit M4.

Results

α Subunit

Figure 1 shows an analysis of one M4 residue, C418 of the α subunit. This side chain is in the middle of the bilayer and projects into the lipid (Blanton and Cohen, 1992, 1994) (Figures 1A and 2). Five mutations of αC418

*Correspondence: auerbach@buffalo.edu

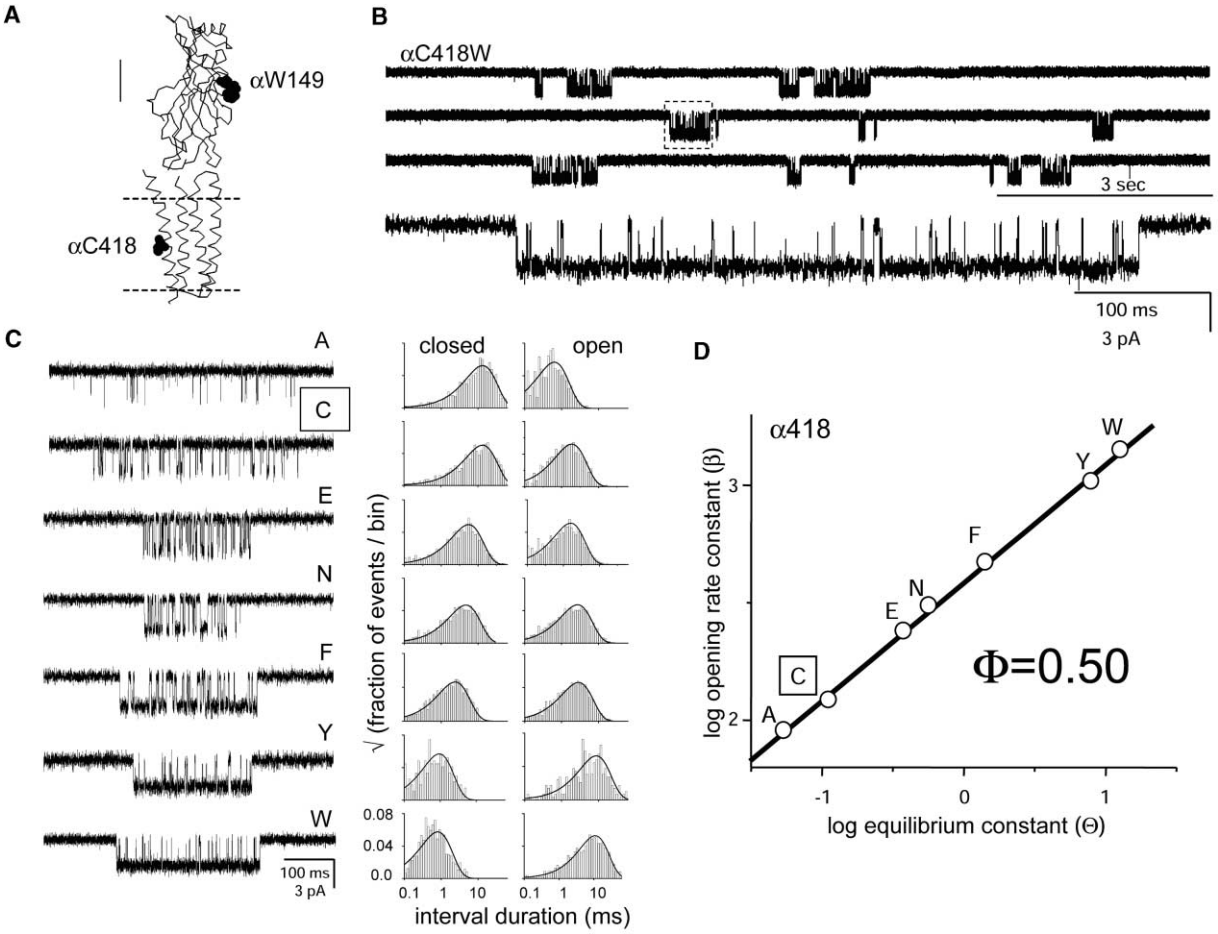

Figure 1. Kinetic Analysis of Residue αC418

(A) The location of C418 in the M4 segment of the AChR α subunit. The extracellular (1I9B.pdb) (Brejc et al., 2002) and transmembrane (1OED.pdb) (Miyazawa et al., 2003) domains were juxtaposed without any detailed modeling. αW149 is at the transmitter binding site; dotted lines show the approximate boundaries of the membrane. Calibration is for the extracellular domain (1.6 nm).

(B) Continuous, low time-resolution view of αC418W single-channel currents elicited by saturating concentration (20 mM) of the weak agonist choline (low-pass filtered at 2 kHz for clarity). In the continued presence of a saturating concentration of agonist, AChRs can adopt closed (low affinity, nonconducting), open (high-affinity, conducting), or desensitized (high-affinity, nonconducting) conformations. The openings (down) are clustered, with silent periods between clusters reflecting long-lived sojourns in desensitized states. Within a cluster, one AChR fluctuates between closed and open conformations. Each cluster reflects the activity of a single AChR, although there are many (~10) present in each patch. On the bottom is the boxed cluster shown on an expanded time scale.

(C) Example clusters from six αC418 constructs (wild-type is boxed) and the corresponding open and closed interval duration histograms. Typically, ~50 clusters and ~3000 intervals were analyzed for each patch. Solid lines are drawn from the optimal rate constants of a closed↔open kinetic model.

(D) REFER plot for α418. Each point is the mean of 3–6 patches. The ϕ value is 0.50 ± 0.01 over a 234-fold range of Θ values.

(E, N, F, W, and Y) increased and one (A) modestly decreased the diliganded gating equilibrium constant (Θ). We interpret a change in Θ following a mutation to indicate that the local environment of the mutated side chain differs between the C and the O conformations, i.e., that the residue (or its environment) moved. The largest effect was a 114-fold increase in Θ with the construct αC418W, which had previously been studied in AChRs (Li et al., 1992; Ortiz-Miranda et al., 1997; Tamamizu et al., 1999).

The changes in Θ arose from inverse and approximately equal-magnitude changes in the apparent closing- and opening-rate constants (Figure 1C). We used rate-equilibrium free energy relationship (REFER) analysis to estimate ϕ, a fraction between 0 and 1 that quantifies the extent to which the perturbed region at the gating reaction transition state resembles the O conformation (see Experimental Procedures). The REFER for position α418 is linear with a slope (ϕ) of 0.50 ± 0.01 (mean ± SD; Figure 1D). This indicates that the closed-to-open switch in conformation of this side chain occurs near the middle of the gating reaction.

Five additional positions were probed in the αM4 segment, using a total of 29 different constructs (Figure 2; Table 1). The sensitivity in Θ was larger for the upper three residues (approximately 42-, 23-, and 234-fold changes) compared to the lower three residues (approximately 4-, 2-, and 5-fold changes) (Figure 6D; Table 1).

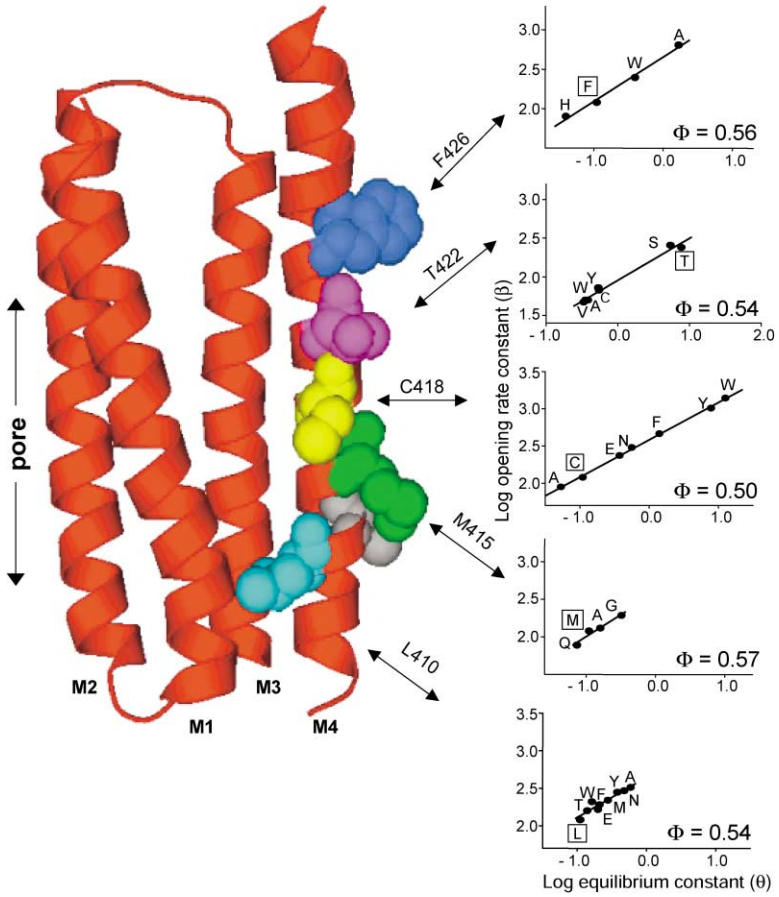

Figure 2. REFER Analyses of αM4

At left is the structure of the α subunit transmembrane domain showing the M1–M4 transmembrane segments (1OED.pdb) (Miyazawa et al., 2003). The probed residues were αF426 (blue), αT422 (magenta), αC418 (yellow), αM415 (green), αG412 (gray), and αL410 (cyan). On the right are REFER plots for each of the probed residues. Each point is the mean of ≥3 patches. The plot for αG412 is not shown because all mutant side chains (A, E, and W) had wild-type gating behavior.

We did not consider the ϕ value of position αG412 to be significant because the fold-change in Θ was <3. ϕ values for all of the other probed positions in αM4 (Figure 2) were remarkably similar and ranged only from 0.50 to 0.57 (mean = 0.54). Because ϕ values illuminate the relative sequence of events during a reaction (Fersht et al., 1992), we conclude that αM4 moves near the middle of the gating reaction, after the α subunit extracellular domain ($\phi > 0.80$) (Chakrapani et al., 2003, 2004; Grosman et al., 2000b) but before the δ subunit M2 segment ($\phi < 0.32$) (Cymes et al., 2002). The consistency of the αM4 ϕ values suggests that during channel opening this segment moves synchronously, i.e., as a rigid body (see Discussion).

Bouzat et al. (2000) carried out a detailed kinetic analysis of αT422 mutants using ACh as the agonist. In order to test the possibility that the nature of the agonist might influence the ϕ values, we recast their rate constant in the form of a REFER plot and examined the same mutational series with choline as the agonist. Because these mutations result in a reduction in Θ, we incorporated a distant, background mutation (δS268N) that by itself increases Θ ~100-fold but has no other significant effects (Grosman and Auerbach, 2000). The ϕ value using ACh was 0.50 ± 0.09 and that with choline was 0.54 ± 0.04. These values are indistinguishable, which leads us to conclude that the agonist per se does not influence the ϕ value.

Figure 3 shows a comparison of ϕ values for the αM4 and δM2 transmembrane segments. In αM4, the average ϕ value is 0.54 throughout, whereas in δM2 the outer half has an average ϕ value of 0.32, while the inner half has an average ϕ value of −0.07. This suggests that during gating αM4 moves as a single, rigid body, whereas δM2 moves as two discrete gating blocks.

α Subunit Hybrids

AChRs have two α subunits that reside in distinct molecular environments. In the vicinity of the transmitter binding sites, mutations of the different α subunits have been shown to make unequal contributions to the gating equilibrium constant. For example, the change in Θ that occurs upon mutation of residue αD200N (Akk et al., 1996) and αD97A (Chakrapani et al., 2003) in one of the α subunits is ~5-fold larger than that in the other α subunit. However, Bouzat et al. (1998) observed only one open time constant for hybrid AChRs, consisting of one wild-type (wt) and one mutated αM4 residue (T422A), which suggests that these two membrane domain mutations make equal and independent contributions to gating (Bouzat et al., 1998). We extended these studies by measuring the opening and closing rate constants for hybrid AChRs in which only one of the two α subunit's M4 domains was mutated.

In cells that were transfected with both wt and αC418W subunit cDNAs (along with wt β, ϵ, and δ), three kinetically distinct populations of clusters were apparent (Figures 4A and 4B). One had the behavior of wt AChRs

Table 1. Gating Rate and Equilibrium Constants

Position	Side Chain	Opening Rate Constant (s^{-1})	Closing Rate Constant (s^{-1})	Equilibrium Constant (Θ)	Θ Ratio (mut/wt)	N
Wild-type	—	120 ± 5.8	1086 ± 67.8	0.11 ± 0.01	1.0	6
α Subunit						
L410 (2′)	T	159 ± 22.6	1136 ± 105.9	0.14 ± 0.04	1.3	4
	W	208 ± 7.16	1272 ± 60.9	0.16 ± 0.06	1.5	3
	E	164 ± 11.5	825 ± 31.7	0.20 ± 0.02	1.8	4
	F	191 ± 24.1	909 ± 124.0	0.21 ± 0.04	1.9	5
	M	219 ± 40.6	786 ± 98.9	0.28 ± 0.08	2.5	3
	Y	280 ± 15.7	736 ± 24.5	0.38 ± 0.01	3.5	3
	N	294 ± 9.3	613 ± 76.4	0.48 ± 0.06	4.4	3
	A	323 ± 26.6	546 ± 61.3	0.59 ± 0.08	5.4	5
M415 (7′)	Q	78 ± 3.9	1049 ± 88.1	0.07 ± 0.008	0.6	3
	A	131 ± 6.8	818 ± 120.6	0.16 ± 0.03	1.5	4
	G	193 ± 6.5	595 ± 55.9	0.32 ± 0.03	2.9	5
C418 (10′)	A	89 ± 18.3	1661 ± 21.0	0.05 ± 0.01	0.5	3
	E	236 ± 17.9	630 ± 20.1	0.37 ± 0.03	3.4	4
	N	302 ± 35.6	536 ± 85.3	0.56 ± 0.06	5.1	3
	F	462 ± 13.5	328 ± 26.7	1.41 ± 0.12	12.8	3
	Y	1019 ± 149.2	130 ± 3.6	7.84 ± 0.97	71.3	3
	W	1391 ± 132.9	110 ± 8.3	12.65 ± 1.57	115.0	4
C418 hybrid	W	443 ± 22.9	405 ± 31.8	1.1 ± 0.03	10.0	11
T422(14′)[a]	V	47 ± 7.4	140 ± 7.5	0.34 ± 0.07	3.1	4
	W	50 ± 2.8	141 ± 19.8	0.35 ± 0.05	3.2	3
	A	50 ± 6.0	130 ± 23.6	0.38 ± 0.07	3.5	6
	Y	72 ± 16.4	134 ± 6.8	0.54 ± 0.16	4.9	3
	C	67 ± 3.1	122 ± 11.2	0.55 ± 0.04	5.0	5
	S	256 ± 20.9	47 ± 8.4	5.40 ± 0.67	49.1	4
	T	239 ± 25.5	31 ± 3.17	7.70 ± 0.77	70.0	3
F426 (18′)	H	80 ± 6.5	2020 ± 119.7	0.04 ± 0.001	0.34	3
	W	249 ± 27.1	632 ± 36.4	0.39 ± 0.04	3.5	3
	A	642 ± 55.7	383 ± 28.2	1.70 ± 0.05	15.5	3
β Subunit						
T464 (10′)	A	110 ± 12.0	1961 ± 234.4	0.06 ± 0.01	0.5	3
	W	111 ± 5.8	556 ± 21.5	0.20 ± 0.007	1.8	3
	I	130 ± 1.7	389 ± 14.8	0.33 ± 0.01	3.0	4
	M	150 ± 6.1	304 ± 24.1	0.49 ± 0.04	4.5	3
	F	172 ± 15.8	301 ± 19.7	0.57 ± 0.08	5.2	4
ε Subunit						
S451 (14′)	H	61 ± 5.5	894 ± 21.5	0.07 ± 0.008	0.6	3
	V	93 ± 2.6	1396 ± 317.1	0.07 ± 0.01	0.6	5
	L	39 ± 3.4	370 ± 23.7	0.11 ± 0.007	1	5
	E	112 ± 4.6	574 ± 22.9	0.19 ± 0.003	1.7	3
	W	153 ± 11.6	140 ± 4.4	1.09 ± 0.11	9.9	4
	A	225 ± 24.9	120 ± 9.4	1.88 ± 0.40	17.1	4

The rate constants (±SE) were obtained in the presence of saturating concentration (20 mM) of choline. The reported values have not been corrected for channel block by agonist, which reduced the closing rate constant by ~2-fold and increased the equilibrium constant by ~2-fold. The hybrid had one wild-type and one mutated α subunit. N represents the number of patches (typically, >50 clusters and >2000 intervals from each patch were used for the rate constant estimates). ϕ values were not determined for 14 residues (49 mutants) because the substitutions produced a <6-fold range in the gating equilibrium constant: αG412(4′)→A,E,W; βF456(2′)→T,A; βF460(6′)→A,E,S; βG467(13′)→H,W,L; βF472(18′)→D,G,H; εC439(2′)→A,H,W,Y; εA443(6′)→E,L,W; εF447(10′)→A,E,H,W; εF455(18′)→A,I,W; δC452(2′)→A,E,H,W; δP458(8′)→A,H,L,S,W; δM460(10′)→A,F,I,N,T; δT464(14′)→A,E,H; δF468(18′)→A,E,R,W.

[a] Residue αT422 was studied with a background mutation in the δ subunit (δS268N).

($\Theta = 0.11$), and one had the behavior of αC418W double mutant AChRs ($\Theta = 11$). The remaining group had an intermediate gating kinetic behavior ($\Theta = 1.1$). We attribute these clusters to hybrid AChRs containing one wt and one mutated α subunit. In the hybrid, the opening rate was ~3.7-fold faster and the closing rate ~2.7-fold slower than the wt. This pattern, a single hybrid class with an increase in Θ (10-fold) that is approximately equal to the square root of the increase of the double mutant (100-fold), indicates that the αC418W mutations in the two subunits have equal and independent effects on gating. Further, the ϕ value for the hybrid was indistinguishable from that of the double mutant (Figure 4C), which suggests that the two α subunits move synchronously during gating, as they do in loop 5 of the extracellular domain (Chakrapani et al., 2003).

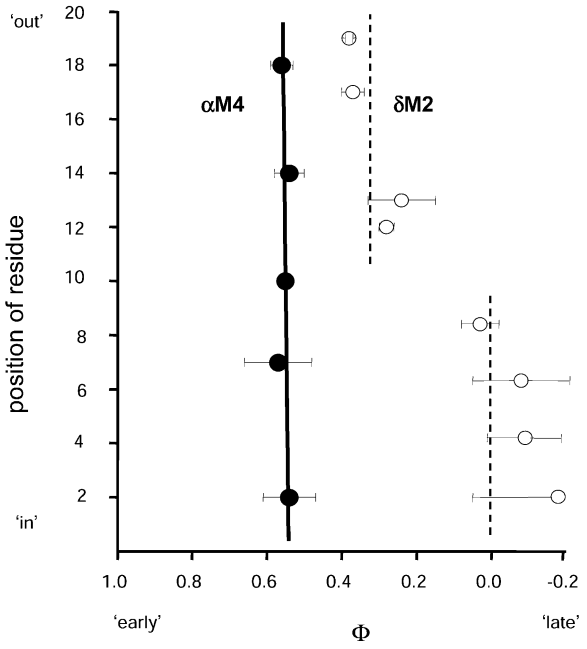

Figure 3. Comparison of ϕ Values in the α Subunit M4 and δ Subunit M2 Segments

The residue positions are according to the primary sequence, starting from the presumed intracellular boundary (1′ is I409 in αM4 and T257 in δM2). In αM4 (represented by filled circles), the ϕ value is consistent throughout (2′–18′; mean = 0.54), whereas in δM2 (represented by open circles) two distinct domains are apparent, with $\phi = 0.32$ (12′–19′) and $\phi = -0.07$ (2′–10′). The M2 values are replotted from Cymes et al., 2002.

β, δ, and ε Subunits

We also probed 15 different positions (58 constructs) in M4 of the non-α subunits (Table 1; Figure 5). In the ε subunit, the only position that was sensitive to mutation was εS451 (14′), which exhibited a 28-fold range in Θ and $\phi = 0.33 \pm 0.12$. In the β subunit, the only position that was sensitive was βT464 (10′), which had a 10-fold range in Θ and $\phi = 0.17 \pm 0.05$. In the δ subunit, Θ was not changed significantly (≥10-fold) by any mutation.

Discussion

We probed 21 different positions in the M4 segments of all of the AChR subunits. The gating rate constants for these 88 different constructs, in combination with previous mutational studies of the M4 segments (Bouzat et al., 2000, 2002; Ortiz-Miranda et al., 1997; Tamamizu et al., 1999), offer a comprehensive picture of the dynamics of M4 in AChR diliganded gating.

ϕ is a fraction that quantifies the extent to which the perturbed region at the transition state resembles the O conformation. We extended this interpretation in three ways, with qualifications. First, we consider residues and domains that have the same ϕ value to be "synchronous" in their gating motion because such sites have progressed to the same extent at the point of our measurement, the transition state. However, we have no information regarding their relative progress up to that point, and thus we do not know that their motions are in fact synchronous throughout. Second, we consider sites that have progressed more ($\phi \rightarrow 1$) or less ($\phi \rightarrow 0$) at the transition state to move "early" or "late" in the reaction, respectively (Fersht, 1999; Fersht et al., 1992).

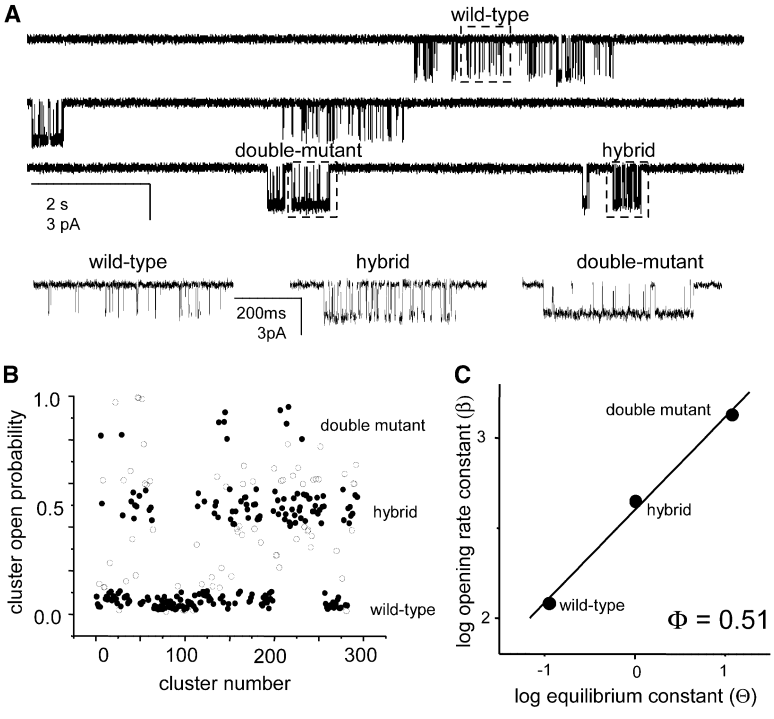

Figure 4. Hybrid αC418W AChRs

Cells were cotransfected with both wt and αC418W α subunit cDNAs (along with wt β, ε, and δ subunit cDNAs) so that patches contained AChRs composed of zero, one, or two mutant α subunits.

(A) Continuous, low-resolution currents (20 mM choline) show heterogeneity in the cluster open probabilities. Each cluster reflects the activity of a single AChR, although AChRs of different subunit composition (wt, single mutant, and double mutant) were present in the patch. The silent periods between clusters reflect intervals when all of the AChRs in the patch were desensitized (see Figure 1B). Below, expanded views of boxed wild-type, hybrid, and double mutant clusters.

(B) Scatter plot of cluster open probabilities (P_o) from one patch showing three distinct populations. The population with the highest P_o corresponds to the double mutant and that with the lowest P_o corresponds to the wild-type. The intermediate populations represent hybrid AChRs. Only the filled symbols were used for estimating the gating rate constants for each population.

(C) REFER plot of wt, hybrid, and double mutant AChRs. The hybrid Θ value indicates that the two α subunit mutations contribute equally to the energy of the gating reaction, and the colinearity of all three constructs suggests that the two α subunit C418 residues move synchronously.

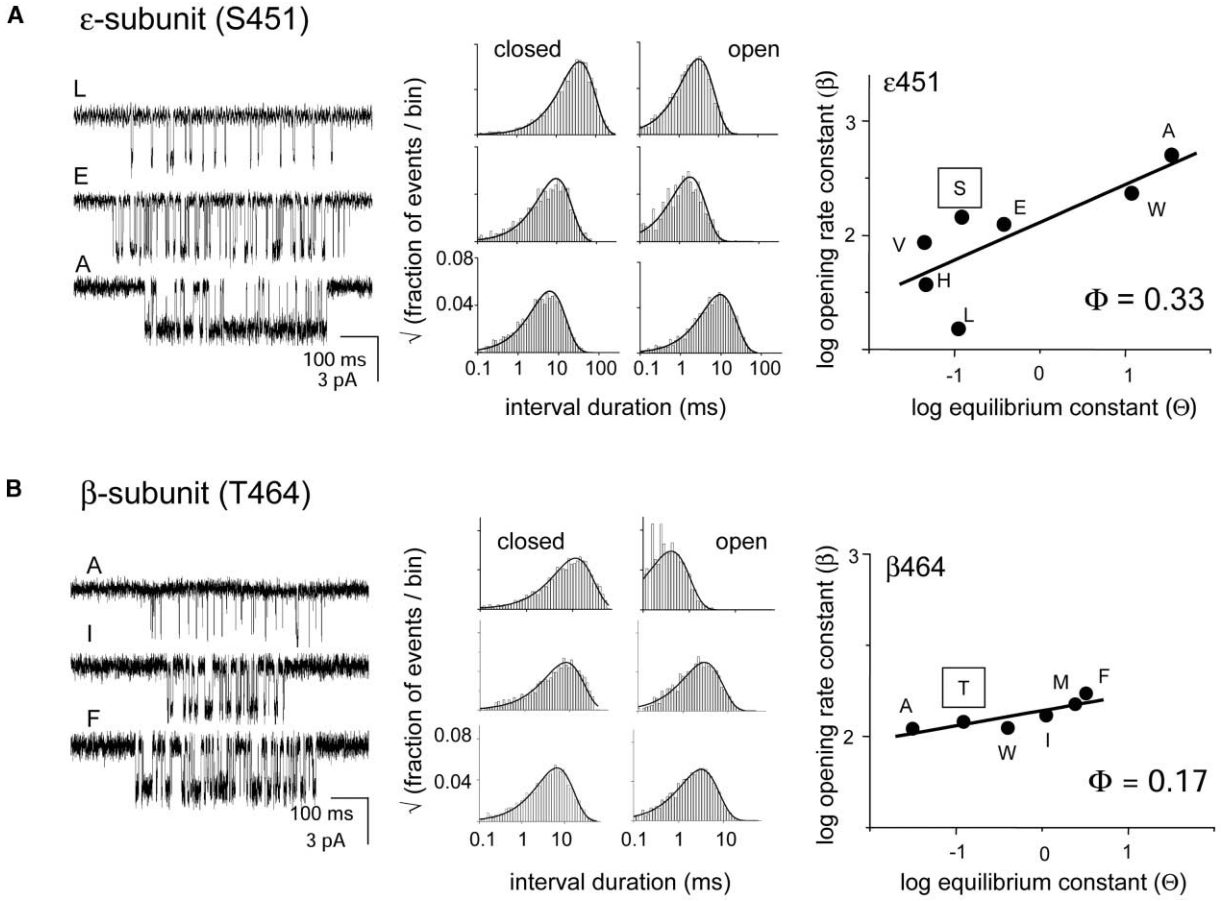

Figure 5. M4 Mutations in Non-α Subunits

(A) Of the five εM4 positions that were mutated (see Table 1), only εS451 was sensitive. On the left are representative clusters from three of the seven εS451 side chains that were examined. In the middle are shown the corresponding open and closed interval duration histograms. At right, the ϕ value for ε451 was 0.33 ± 0.12, encompassing a 28-fold range of Θ values. Each point is the average of 3–5 patches.
(B) Of the five βM4 positions that were mutated (see Table 1), only β464 was sensitive. On the left are representative clusters from three of the six β464 side chains that were examined. In the middle is shown the corresponding open and closed interval duration histograms. At right, the ϕ value for β464 was 0.17 ± 0.05, encompassing a >10-fold range of Θ values. Each point is the average of 3–5 patches. In both REFER plots, the wild-type side chain is boxed.

However, ϕ values only rank the event sequence and, further, do so only in relation to the transition state. The REFER method does not provide information regarding the absolute timing of gating motions, and even the sequence order is lost when the transition state is very early (all ϕ values→0) or late (all ϕ values→1) in the reaction (Grosman, 2003). Third, we consider a contiguous domain within which all residues have the same ϕ value (a "block") to act as a "rigid body." However, our measurements do not provide information about the actual stiffness of such domains. These provisos should be kept in mind when we use the terms synchronous, early/late, and rigid in our interpretation of ϕ values.

Compared to some other regions of the AChR, M4 is not particularly sensitive to mutations insofar as the gating equilibrium constant (Θ) is concerned. More than half of the mutants we examined had wild-type gating behavior, and only five positions exhibited a >10-fold range in Θ (Table 1; Figure 6D). M4 is far from the transmitter binding sites, and previous studies have shown that mutations to this region do not alter the affinity of the closed AChR for agonists (Bouzat et al., 2000). It is therefore likely that the changes in Θ that we observed reflect parallel changes in the unliganded gating equilibrium constant (Chakrapani et al., 2003; Zhou et al., 1999). Interestingly, the M4 mutations both increase and decrease Θ, whereas those in δM2 typically increase Θ (Cymes et al., 2002).

Mutations in the upper half of M4 have a larger effect on Θ compared to those in the lower half (Figure 6D), similar to the pattern observed in δM2 (Cymes et al., 2002). One interpretation of this pattern is that the extent of movement in the outer halves of M2 and M4 is greater than that of their inner halves. Along similar lines, cross-linking studies suggest that the outer portion of the M2 domain of $GABA_A$ receptors moves more than the inner portion during gating (Horenstein et al., 2001). Two features of the M4 pattern, however, suggest that there may be discrete interactions between specific AChR residues and elements of the lipid bilayer (Bouzat et al., 2000; Garbus et al., 2002). First, four of the five sensitive positions in wt AChRs can form hydrogen bonds (S, T,

or C; the exception was αF426). Second, most of the mutations in the outer half (10′ and above) of the β-, ϵ-, and δ-subunit M4 segments did not affect Θ (Table 1). This suggests that the changes in side-chain environment that occur between C and O conformations are mainly in the α subunit and are restricted to discrete loci in the non-α subunits. Note that although a change in Θ implies movement, stable Θ does not necessarily imply a lack of movement because the local environment could move along with the residue. Our results support the notion that molecules in the proximate lipid environment should be considered integral to AChR function (Barrantes, 2002, 2003; Valiyaveetil et al., 2002).

ϕ values provide insight into the dynamics of AChR gating, which to first approximation occurs as a sequence of discrete gating-block movements (Chakrapani et al., 2004). REFER analyses of αM4 show that there is a single ϕ value (∼0.54) throughout its entire length, which indicates that during gating this segment moves as a synchronous unit, that is, as a rigid body. This is in contrast to δM2, which moves as two distinct gating blocks (Cymes et al., 2002) (Figure 3). These observations are consistent with structural analyses that show M4 to be a straight α helix (Blanton and Cohen, 1992, 1994; Miyazawa et al., 2003), whereas M2 has a central, "kinked" region (Unwin, 1993, 1995).

The movement of αM4 fits with the general pattern of diliganded AChR gating occurring as a reversible conformational wave that connects transmitter binding sites and the gate (Grosman et al., 2000b). The ϕ value for αM4 places the movement of this gating domain near the midpoint of the overall reaction. Figure 6A summarizes the sequence of gating block motions in the α subunit. The three gating blocks are TBS/loop5 (ϕ = 0.93), loop7/loop2 (ϕ = 0.80), and M4 (ϕ = 0.54). In addition, a residue that is located in M2 near the interface with loop2 of the extracellular domain (αS269; 27′ position) (Miyazawa et al., 2003) has been probed (ϕ = 0.69) (Grosman et al., 2000a), but the boundaries of this gating domain have not yet been identified. Although the atomic structure of the AChR is not known, we can approximate the distance (parallel to the pore axis) from the middle of these three domains and residue αW149, which forms the base of the ligand binding pocket (Celie et al., 2004). Figure 6B shows the relationship between the gating reaction progress (ϕ) and this distance. In the α subunit, the AChR gating conformational change appears to propagate along the longitudinal axis of the protein at a uniform rate of 0.092 ϕ-unit/nm.

Only one position in each of the β and ϵ subunits was amenable to REFER analysis. Although the ϕ values for these positions are reliable (in the sense that we studied multiple substitutions that spanned a >10-fold range in Θ), the fact that ϕ could be measured only at one position means that we cannot be certain that the entire M4 segment moves as a rigid body (as it does in the α subunit). However, given that these positions were in the middle of the segment and that the structures of M4 are similar in all five subunits, we speculate that these ϕ values reflect those of the entire segment.

Our analysis also provides some information as to the sequence of movements among the five AChR subunits (Figure 6C). In M4, the rank of ϕ values is α(0.54) > ϵ(0.33) > β(0.17), which indicates that α moves first, followed by ϵ and then β, with both α subunits moving in synchrony (see below). This order of movement is the same as was found for perturbations of the M2-M3 extracellular linker in each of the subunits: α(0.69) > ϵ(0.57) > β(0.43) (Grosman et al., 2000a). This sequence may reflect subunit-dependent differences in the initiation/propagation of the isomerization along the longitudinal axis, but could also be influenced by conformational spread in circumferential and radial dimensions. It may be relevant to note that the ϵ subunit contacts two α subunits and moves in advance of the β subunit, which is apposed to only one α subunit.

We can compare our results regarding M4 hybrid AChRs (having one wt and one mutated α subunit) with similar studies of TBS/loop5 hybrid AChRs (Akk et al., 1996; Chakrapani et al., 2003). With respect to their contributions to the gating equilibrium constant in M4, the two α subunits are approximately equal, whereas in the TBS/loop5 domain, one subunit dominates by ∼5-fold. This difference in the energetic contribution to gating (∼1 kcal/mol) may simply arise from a higher degree of similarity in the lipid environments of the two M4 segments compared to those of the TBS/loop domains, which lie at distinct subunit interfaces.

In the hybrid AChRs, residues in both loop5 (Chakrapani et al., 2003) and M4 have similar ϕ values in each of the α subunits. This suggests that these two subunits move synchronously in the gating reaction. This observation is curious, because in both of these domains the α subunits are separated by a distance of >5 nm (Figure 6C). Perhaps our measurements are not sensitive enough to detect a difference in the relative timing of the two α subunits and the apparent synchronicity arises simply from independent, parallel gating behaviors of structures that have comparable initiation loci and propagation mechanisms. However, it is also possible that the two α subunits are synchronized by nongating conformational events that serve to communicate information between the two transmitter binding sites (Demazumder and Dilger, 2001).

It is remarkable that the AChR has so many moving parts. We have defined a gating block as a contiguous structural element that moves as a rigid body, i.e., within which all residues are characterized by the same ϕ value. The two αM4 segments fit this definition, and we speculate that the entire M4 segments of the β and ϵ subunits also move as rigid bodies. So far, ten gating blocks have been identified in the AChR: six in the two α subunits (TBS/loop5, loop2/loop7, M4), one in the β subunit (M4), one in the ϵ subunit (M4), and two in the δ subunit (outer and inner halves of M2). Undoubtedly, more such rigid domains will be revealed, whereas other domains will prove to be more flexible kinematic elements. It appears that, during gating, the block movements are coupled, sequential (according to their ϕ values), and occur by a mechanism that is characterized by Brownian motion (S. Chakrapani and A.L.A., unpublished data). It is also possible that only a subset of domain motions is needed to couple the affinity change of the binding sites with the conductance change of the pore. Further high-resolution mapping of ϕ values and insights into the molecular forces within and between

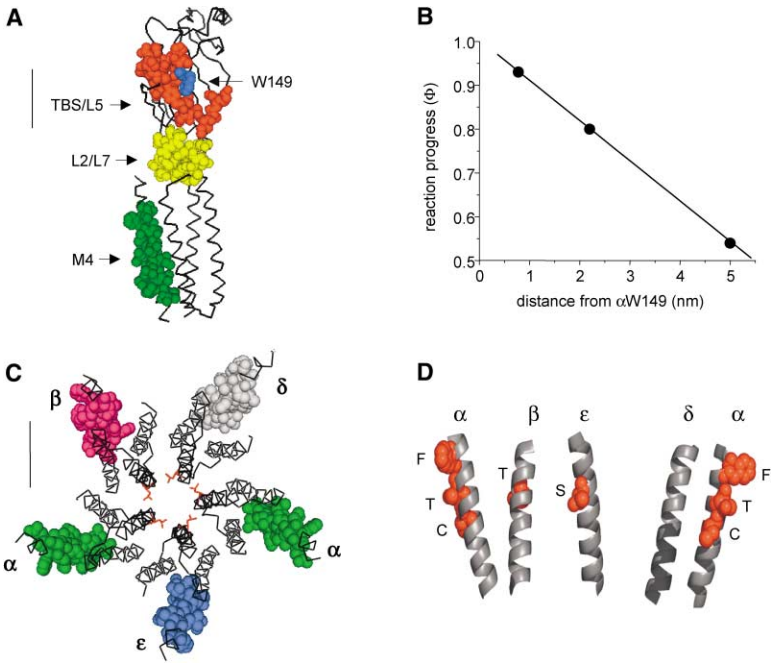

Figure 6. AChR Gating Blocks

(A) The location of TBS/loop5, loop2/loop7, and M4 gating blocks in the AChR α subunit. The extracellular (1I9B.pdb) and transmembrane (1OED.pdb) domains were juxtaposed without any detailed modeling. αW149 is at the transmitter binding site. Calibration (1.6 nm) is for the extracellular domain.

(B) The ϕ values of the gating blocks change uniformly with distance from the transmitter binding site. The slope of the line is 0.092 ϕ-unit/nm.

(C) Extracellular (top-down) view of the transmembrane domain showing the M4 atoms as spheres (calibration, 1.6 nm). The central, M2 leucine (9′) of each subunit is shown in orange. The M4 block in the α subunit moves first (green; $\phi = 0.50$), followed by the ε subunit (blue; $\phi = 0.33$), followed by the β subunit (magenta; $\phi = 0.17$). None of the δ subunit (gray) mutations changed the gating equilibrium constant, which suggests that this domain does not move relative to its local environment during gating. The movements of the two α subunits are synchronous (see Figure 4).

(D) M4 helices from all five subunits, with the residues that were sensitive to mutation (>10-fold change in the gating equilibrium constant) shown in red (see Table 1). There are specific loci of sensitivity that all fall in the outer half of the M4 segment and that in the wild-type are mainly composed of side chains that can participate in a hydrogen bond (C, S, and T).

blocks will help us understand the AChR as a nanomachine.

Experimental Procedures

Mutagenesis and Expression

cDNA of the α, β, δ, and ε subunits of mouse muscle AChRs were generous gifts from Dr. S. Sine (Mayo Foundation, Rochester, MN). All other mutations were engineered using the QuikChange Site-Directed Mutagenesis Kit (Stratagene) protocol. All constructs were confirmed by dideoxy sequencing. In the original cDNAs, the α subunit had an alanine at position 433 in M4. Although this mutation does not affect gating (Salamone et al., 1999), we changed it back to the wild-type valine in order to avoid the possibility of interactions with other M4 mutations.

Human embryonic kidney fibroblast cells (HEK 293) were transiently transfected using calcium phosphate. A total of 3.5 μg of cDNA per 35 mm culture dish in the ratio of 2:1:1:1 (α:β:δ:ε) was administered to the cells for 12 to 15 hr, after which the medium was changed. Electrophysiological recordings commenced ~24 hr later.

Electrophysiology

Recordings were performed in the cell-attached patch configuration at 22°–24°C. The bath and pipette solution was Dulbecco's phosphate-buffered saline containing (mM) 137 NaCl, 0.9 $CaCl_2$, 2.7 KCl, 1.5 KH_2PO_4, 0.5 $MgCl_2$, and 8.1 Na_2HPO_4 (pH 7.3). Agonist was added only to the pipette solution, as indicated. Borosilicate capillaries were used for the patch pipettes, coated with Sylgard (Dow Corning Corp., Midland, MI), and fire polished to a final resistance of 7–10 MΩ. The potential of the pipette was +60 mV, which corresponds to a membrane potential of −60 to −90 mV. Single-channel currents were recorded using a PC-505 amplifier (Warner Instrument Corp., Hamden, CT) with low-pass filtering at 20 kHz. The currents were digitized at a sampling frequency of 50 kHz using a National Instruments SCB-68 acquisition board and QUB software (www.qub.buffalo.edu).

Because many of the M4 mutations increased the gating equilibrium constant, we used the low-efficacy agonist choline at saturating concentration (20 mM) to estimate the channel-opening rate constant (Zhou et al., 1999). Because this concentration is approximately the equilibrium dissociation constant for fast, open-channel block by choline (Grosman and Auerbach, 2000), the single-channel current amplitude was reduced and the apparent open-channel lifetime was increased, each by ~2-fold compared to experiments at low choline concentrations, where block is negligible. M4 is distant from the pore, and we suspected that the block-induced increase in open-channel lifetime was the same for all constructs. To check this, we measured the closing rate constant using 200 μM choline, a concentration where channel block is insignificant. The closing rate constant was estimated as [the inverse of the open time − 200 s^{-1}], which takes into account the rate constants for dissociation of choline from open AChRs (Cymes et al., 2002) and desensitization (Elenes and Auerbach, 2002). In these experiments (15 patches from 3 different α subunit M4 mutant constructs: αL410A, αF426H, and αF426W), the ratio of the closing rate constant measured at 20 mM and the inverse of the apparent open channel lifetime at 200 μM choline was 0.50 ± 0.1. This suggests that M4 mutations do not alter the kinetics or equilibrium constant of open-channel block by choline. The values reported in the text and Table 1 are the *apparent* closing rate constants measured using 20 mM choline, which are ~ half of the true closing rate constants.

Kinetic Analyses

All kinetic analyses were carried out using QuB software (www.qub.buffalo.edu). At 20 mM choline, openings occur in clusters, with long gaps between clusters reflecting intervals during which all of the AChRs in the patch are desensitized (Figure 1). Clusters of openings were selected either by eye or by invoking a critical closed-interval duration (t_{crit}) of 15–50 ms. The selected currents were further low-pass filtered to yield an effective analysis bandwidth of 12 kHz and were idealized into noise-free intervals with the segmental k-means algorithm (SKM) (Qin, 2004) using a C↔O model with a starting rate constant of 10 s^{-1}. The apparent opening and closing rate constants were estimated from these idealized sequences of intervals using a maximum-likelihood algorithm (MIL) (Qin et al., 1997, 2000) after imposing a "dead time" of 33–75 μs. We used a two-state, C↔O model with a starting rate constant estimate of 100 s^{-1}. The apparent gating equilibrium constant (Θ) was computed as the ratio of the opening rate constant (β) and the *apparent* closing

rate constant (α^*). Because of channel block, in the rate-equilibrium plots and tables the diliganded gating equilibrium constants are $\sim$2-fold larger than what they would be without channel block.

Rate-Equilibrium Free Energy Relationships

In the presence of a saturating concentration of agonist and with our imposed dead time, AChR gating appeared as a two-state reaction. In order to decipher the sequence of conformational changes that constitutes this step, we probed the intermediate states of this reaction. These are the conformations between the stable, C and O end states that are too brief to be detected directly. We did this using rate-equilibrium free energy relationship (REFER) analysis (Fersht, 1999; Grosman, 2002; Leffler and Grunwald, 1963), where the correlation between rate and equilibrium constant for series of point mutants, ϕ, measures the extent to which the perturbed region at the reaction transition state resembles the O conformation. ϕ is a fraction between 1 and 0, with $\phi = 1$ implying an open-like character and, hence, that the perturbed site moved relatively early in the reaction.

Hybrid AChRs

Cells were transfected with both wild-type and mutant (C418W) α subunit cDNAs in a 1:10 ratio, together with wild-type β, ϵ, and δ subunit cDNAs. Most recordings showed populations of clusters (11 out of 14 patches) that could be distinguished according to the cluster open probability (P_{open}) as arising from wild-type, hybrid (containing one wild-type and one mutant α subunit), or double mutant AChRs. Clusters were either selected by eye or defined using a τ_{crit} of 50 ms and were segregated into separate populations for subsequent kinetic analyses using the SKM algorithm with only P_{open} as the discrimination criterion. Clusters that had P_{open} values that were $>$1 SD removed from the corresponding population mean were not selected for further analysis.

Acknowledgments

We thank Mary Teeling and Birte Steidl for technical assistance. This work was supported by NS-23513 to A.L.A.

Received: June 2, 2004
Revised: August 3, 2004
Accepted: August 4, 2004
Published: October 5, 2004

References

Akk, G., Sine, S., and Auerbach, A. (1996). Binding sites contribute unequally to the gating of mouse nicotinic alpha D200N acetylcholine receptors. J. Physiol. *496*, 185–196.

Auerbach, A. (2003). Life at the top: the transition state of AChR gating. Sci. STKE *2003*, re11.

Barrantes, F.J. (2002). Lipid matters: nicotinic acetylcholine receptor-lipid interactions (Review). Mol. Membr. Biol. *19*, 277–284.

Barrantes, F.J. (2003). Modulation of nicotinic acetylcholine receptor function through the outer and middle rings of transmembrane domains. Curr. Opin. Drug Discov. Dev. *6*, 620–632.

Blanton, M.P., and Cohen, J.B. (1992). Mapping the lipid-exposed regions in the Torpedo californica nicotinic acetylcholine receptor. Biochemistry *31*, 3738–3750.

Blanton, M.P., and Cohen, J.B. (1994). Identifying the lipid-protein interface of the Torpedo nicotinic acetylcholine receptor: secondary structure implications. Biochemistry *33*, 2859–2872.

Blount, P., and Merlie, J.P. (1989). Molecular basis of the two nonequivalent ligand binding sites of the muscle nicotinic acetylcholine receptor. Neuron *3*, 349–357.

Bouzat, C., Roccamo, A.M., Garbus, I., and Barrantes, F.J. (1998). Mutations at lipid-exposed residues of the acetylcholine receptor affect its gating kinetics. Mol. Pharmacol. *54*, 146–153.

Bouzat, C., Barrantes, F., and Sine, S. (2000). Nicotinic receptor fourth transmembrane domain: hydrogen bonding by conserved threonine contributes to channel gating kinetics. J. Gen. Physiol. *115*, 663–672.

Bouzat, C., Gumilar, F., del Carmen Esandi, M., and Sine, S.M. (2002). Subunit-selective contribution to channel gating of the M4 domain of the nicotinic receptor. Biophys. J. *82*, 1920–1929.

Brejc, K., van Dijk, W.J., Smit, A.B., and Sixma, T.K. (2002). The 2.7 A structure of AChBP, homologue of the ligand-binding domain of the nicotinic acetylcholine receptor. Novartis Found. Symp. *245*, 22–29; discussion 29–32, 165–168.

Celie, P.H., van Rossum-Fikkert, S.E., van Dijk, W.J., Brejc, K., Smit, A.B., and Sixma, T.K. (2004). Nicotine and carbamylcholine binding to nicotinic acetylcholine receptors as studied in AChBP crystal structures. Neuron *41*, 907–914.

Chakrapani, S., Bailey, T.D., and Auerbach, A. (2003). The role of loop 5 in acetylcholine receptor channel gating. J. Gen. Physiol. *122*, 521–539.

Chakrapani, S., Bailey, T.D., and Auerbach, A. (2004). Gating dynamics of the acetylcholine receptor extracellular domain. J. Gen. Physiol. *123*, 341–356.

Changeux, J.P., and Edelstein, S.J. (1998). Allosteric receptors after 30 years. Neuron *21*, 959–980.

Chiara, D.C., and Cohen, J.B. (1997). Identification of amino acids contributing to high and low affinity d-tubocurarine sites in the Torpedo nicotinic acetylcholine receptor. J. Biol. Chem. *272*, 32940–32950.

Cymes, G.D., Grosman, C., and Auerbach, A. (2002). Structure of the transition state of gating in the acetylcholine receptor channel pore: a phi-value analysis. Biochemistry *41*, 5548–5555.

Demazumder, D., and Dilger, J.P. (2001). The kinetics of competitive antagonism by cisatracurium of embryonic and adult nicotinic acetylcholine receptors. Mol. Pharmacol. *60*, 797–807.

Elenes, S., and Auerbach, A. (2002). Desensitization of diliganded mouse muscle nicotinic acetylcholine receptor channels. J. Physiol. *541*, 367–383.

Fersht, A. (1999). Structure and Mechanism in Protein Science: A Guide to Enzyme Catalysis and Protein Folding (New York: W.H. Freeman).

Fersht, A.R., Matouschek, A., and Serrano, L. (1992). The folding of an enzyme. I. Theory of protein engineering analysis of stability and pathway of protein folding. J. Mol. Biol. *224*, 771–782.

Garbus, I., Roccamo, A.M., and Barrantes, F.J. (2002). Identification of threonine 422 in transmembrane domain alpha M4 of the nicotinic acetylcholine receptor as a possible site of interaction with hydrocortisone. Neuropharmacology *43*, 65–73.

Grosman, C. (2002). Linear free-energy relationships and the dynamics of gating in the acetylcholine receptor channel - A Phi-value analysis of an allosteric transition at the single-molecule level. J. Biol. Phys. *28*, 267–277.

Grosman, C. (2003). Free-energy landscapes of ion-channel gating are malleable: changes in the number of bound ligands are accompanied by changes in the location of the transition state in acetylcholine-receptor channels. Biochemistry *42*, 14977–14987.

Grosman, C., and Auerbach, A. (2000). Asymmetric and independent contribution of the second transmembrane segment 12′ residues to diliganded gating of acetylcholine receptor channels: a single-channel study with choline as the agonist. J. Gen. Physiol. *115*, 637–651.

Grosman, C., Salamone, F.N., Sine, S.M., and Auerbach, A. (2000a). The extracellular linker of muscle acetylcholine receptor channels is a gating control element. J. Gen. Physiol. *116*, 327–340.

Grosman, C., Zhou, M., and Auerbach, A. (2000b). Mapping the conformational wave of acetylcholine receptor channel gating. Nature *403*, 773–776.

Horenstein, J., Wagner, D.A., Czajkowski, C., and Akabas, M.H. (2001). Protein mobility and GABA-induced conformational changes in GABA(A) receptor pore-lining M2 segment. Nat. Neurosci. *4*, 477–485.

Jackson, M.B. (1989). Perfection of a synaptic receptor: kinetics

and energetics of the acetylcholine receptor. Proc. Natl. Acad. Sci. USA *86*, 2199–2203.

Karlin, A., and Akabas, M.H. (1995). Toward a structural basis for the function of nicotinic acetylcholine receptors and their cousins. Neuron *15*, 1231–1244.

Lee, Y.H., Li, L., Lasalde, J., Rojas, L., McNamee, M., Ortiz-Miranda, S.I., and Pappone, P. (1994). Mutations in the M4 domain of Torpedo californica acetylcholine receptor dramatically alter ion channel function. Biophys. J. *66*, 646–653.

Leffler, J.E., and Grunwald, E. (1963). Rates and Equilibria of Organic Reactions as Treated by Statistical, Thermodynamic, and Extrathermodynamic Methods (New York: Wiley).

Li, L., Lee, Y.H., Pappone, P., Palma, A., and McNamee, M.G. (1992). Site-specific mutations of nicotinic acetylcholine receptor at the lipid-protein interface dramatically alter ion channel gating. Biophys. J. *62*, 61–63.

Miyazawa, A., Fujiyoshi, Y., and Unwin, N. (2003). Structure and gating mechanism of the acetylcholine receptor pore. Nature *423*, 949–955.

Ortiz-Miranda, S.I., Lasalde, J.A., Pappone, P.A., and McNamee, M.G. (1997). Mutations in the M4 domain of the Torpedo californica nicotinic acetylcholine receptor alter channel opening and closing. J. Membr. Biol. *158*, 17–30.

Qin, F. (2004). Restoration of single-channel currents using the segmental k-means method based on hidden Markov modeling. Biophys. J. *86*, 1488–1501.

Qin, F., Auerbach, A., and Sachs, F. (1997). Maximum likelihood estimation of aggregated Markov processes. Proc. R. Soc. Lond. B. Biol. Sci. *264*, 375–383.

Qin, F., Auerbach, A., and Sachs, F. (2000). A direct optimization approach to hidden Markov modeling for single channel kinetics. Biophys. J. *79*, 1915–1927.

Salamone, F.N., Zhou, M., and Auerbach, A. (1999). A re-examination of adult mouse nicotinic acetylcholine receptor channel activation kinetics. J. Physiol. *516*, 315–330.

Sine, S.M. (2002). The nicotinic receptor ligand binding domain. J. Neurobiol. *53*, 431–446.

Sine, S.M., and Claudio, T. (1991). Gamma- and delta-subunits regulate the affinity and the cooperativity of ligand binding to the acetylcholine receptor. J. Biol. Chem. *266*, 19369–19377.

Tamamizu, S., Lee, Y., Hung, B., McNamee, M.G., and Lasalde-Dominicci, J.A. (1999). Alteration in ion channel function of mouse nicotinic acetylcholine receptor by mutations in the M4 transmembrane domain. J. Membr. Biol. *170*, 157–164.

Unwin, N. (1993). Nicotinic acetylcholine receptor at 9 A resolution. J. Mol. Biol. *229*, 1101–1124.

Unwin, N. (1995). Acetylcholine receptor channel imaged in the open state. Nature *373*, 37–43.

Unwin, N. (2000). The Croonian Lecture 2000. Nicotinic acetylcholine receptor and the structural basis of fast synaptic transmission. Philos. Trans. R. Soc. Lond. B Biol. Sci. *355*, 1813–1829.

Valiyaveetil, F.I., Zhou, Y., and MacKinnon, R. (2002). Lipids in the structure, folding, and function of the KcsA K+ channel. Biochemistry *41*, 10771–10777.

Zhou, M., Engel, A.G., and Auerbach, A. (1999). Serum choline activates mutant acetylcholine receptors that cause slow channel congenital myasthenic syndromes. Proc. Natl. Acad. Sci. USA *96*, 10466–10471.